Tumstatin Peptide, an Inhibitor of Angiogenesis, Prevents Glomerular Hypertrophy in the Early Stage of Diabetic Nephropathy

Yoshihiko Yamamoto, Yohei Maeshima, Hiroyuki Kitayama, Shinji Kitamura, Yuki Takazawa, Hitoshi Sugiyama, Yasushi Yamasaki, and Hirofumi Makino

In the early stage of diabetic nephropathy (one of the major microvascular complications of diabetes) glomerular hyperfiltration and hypertrophy are observed. It is clinically important to regulate glomerular hypertrophy for preventing glomerulosclerosis. The number of glomerular endothelial cells is known to be increased in diabetic nephropathy associated with enlarged glomerular tufts, suggesting that the mechanism is similar to that of angiogenesis. Tumstatin peptide is an angiogenesis inhibitor derived from type IV collagen and inhibits in vivo neovascularization induced by vascular endothelial growth factor (VEGF), one of the mediators of glomerular hypertrophy in diabetic nephropathy. Here, we show the effect of tumstatin peptide in inhibiting alterations in early diabetic nephropathy. Glomerular hypertrophy, hyperfiltration, and albuminuria were suppressed by tumstatin peptide (1 mg/kg) in streptozotocin-induced diabetic mice. Glomerular matrix expansion, the increase of total glomerular cell number and glomerular endothelial cells (CD31 positive), and monocyte/macrophage accumulation was inhibited by tumstatin peptide. Increase in renal expression of VEGF, flk-1, and angiopoietin-2, an antagonist of angiopoietin-1, was inhibited by tumstatin treatment in diabetic mice. Alteration of glomerular nephrin expression, a podocyte protein crucial for maintaining glomerular filtration barrier, was recovered by tumstatin in diabetic mice. Taken together, these results demonstrate the potential use of antiangiogenic tumstatin peptide as a novel therapeutic agent in early diabetic nephropathy.
Diabetes **53:1831–1840, 2004**

Diabetic nephropathy is complicated in 30–40% of patients with type 2 diabetes and is the most common pathological disorder predisposing end-stage renal diseases in Japan and in the western world (1). Hyperglycemia is involved in the progression of diabetic nephropathy, and early alterations in diabetic nephropathy include glomerular hyperfiltration, glomerular and tubular epithelial hypertrophy, and the development of microalbuminuria (2). These early alterations are followed by the development of glomerular basement membrane thickening, the accumulation of extracellular matrix components in mesangium as well as in the interstitium, and the increase of urinary albumin excretion, eventually leading to glomerulosclerosis and progressive loss of renal function (3,4). The involvement of angiotensin II, insulin-like growth factor-1, and transforming growth factor (TGF)-β1 in the development of diabetic nephropathy have been reported (5,6). Vascular endothelial growth factor (VEGF) is one of the potent stimulators of angiogenesis with the capacity to promote endothelial cell proliferation, migration, and tube formation (7). VEGF also induces vascular permeability and endothelium-dependent vasodilatation in association with endothelium-derived nitric oxide (8). The protein and mRNA level of VEGF and the high-affinity receptor of VEGF, flk-1/KDR, were reported to be upregulated in the early as well as the late stage of experimental diabetic nephropathy (9,10). Recent animal studies (11,12) utilizing neutralizing anti-VEGF antibody further demonstrated the involvement of this factor in early glomerular hypertrophy and mesangial matrix accumulation in the progressive stage of diabetic nephropathy.

Angiopoietin (Ang)-1, a major physiological ligand for Tie-2 receptor, is responsible for the recruitment and stable attachment of pericytes resulting in vascular maturation in the process of angiogenesis (13). Ang-2 competitively inhibits the binding of Ang-1 to Tie-2, acting like a natural antagonist and rendering blood vessels "unstable" (14). During kidney development, Ang-1, Ang-2, and Tie-2 are highly expressed and play pivotal roles in the maturation of glomeruli as well as renal blood vessels (15). The involvement of Ang-1, Ang-2, and Tie-2 in the progression of diabetic nephropathy has yet to be elucidated.

Nephrin, a recently found podocyte protein, is crucial for the integrity of interpodocyte slit membrane structure and maintenance of an intact filtration barrier (16). In diabetic nephropathy, protein level of nephrin decreases possibly through the loss of nephrin into urine due to synthesis of the splice variant isoform of nephrin lacking a transmembrane domain (17–19).

Angiogenesis, the development of new blood vessels from preexisting ones (20), is involved in physiological

From the Department of Medicine and Clinical Science, Okayama University Graduate School of Medicine and Dentistry, Okayama, Japan.

Address correspondence and reprint requests to Dr. Yohei Maeshima, Assistant Professor of Medicine, Department of Medicine and Clinical Science, Okayama University Graduate School of Medicine and Dentistry, 2-5-1 Shikata-cho, Okayama, 700-8558, Japan. E-mail: ymaeshim@md.okayama-u.ac.jp.

Received for publication 7 February 2004 and accepted in revised form 5 April 2004.

Ang, angiopoietin; Ccr, creatinine clearance; GAPDH, glyceraldehyde-3-phosphate dehydrogenase; PAS, periodic acid-Schiff; PI, phosphatidylinositol; STZ, streptozotocin; TGF, transforming growth factor; UACR, urinary albumin–to–creatinine ratio; VEGF, vascular endothelial growth factor.

events such as wound repair, but uncontrolled neovascularization is associated with a number of pathological disorders including tumor growth and rheumatoid arthritis as well as diabetic retinopathy (21).

A previous study (22) demonstrated that the increased glomerular filtration surface in diabetic nephropathy resulted from the formation of new glomerular capillaries in accordance with a slight elongation of the preexisting capillaries, analogous to the changes observed in pathologic diabetic retinopathy. That study was suggestive of the involvement of angiogenesis in the development of glomerular alterations in diabetic nephropathy similar to diabetic retinopathy.

Type IV collagen is expressed as six distinct α-chains [namely α1-α6 (23)], assembles into triple helices, and forms a network. These α-chains consist of the NH_2-terminal 7S domain, the middle triple helical domain, and the COOH-terminal globular noncollagenous domain (NC1) (24). Tumstatin, the NC1 domain of the α3 chain of human type IV collagen, possesses potent antiangiogenic activity (25). Tumstatin can block in vivo neovascularization induced by VEGF in mice, and the T7- and T8-peptides encompassing 25 amino acids in the NH_2-terminus portion of tumstatin possess antiangiogenic capacity (26,27). Through its interaction with αVβ3-integrin, tumstatin inhibits activation of focal adhesion kinase (FAK), phosphatidylinositol (PI)-3 kinase, Akt, and mTOR and prevents the dissociation of the eIF4E/4E-BP1 complex, resulting in the inhibition of cap-dependent protein translation in endothelial cells (28,29).

In the present study, we demonstrate the therapeutic effect of tumstatin peptide in ameliorating alterations in the early stage of diabetic nephropathy induced by streptozotocin (STZ) in mice. Treatment with tumstatin peptide markedly suppressed glomerular hypertrophy, hyperfiltration, and urinary albumin excretion as well as the accumulation of mesangial matrix. These effects were supposed to be mediated through downregulation of proangiogenic factors, VEGF and Ang-2, and the recovery of nephrin expression.

RESEARCH DESIGN AND METHODS

Induction of diabetes and experimental protocols. The experimental protocol was approved by the Animal Ethics Review Committee of Okayama University Graduate School of Medicine and Dentistry. Female C57BL6 mice were fed a standard pellet laboratory diet and were provided with water ad libitum. Diabetes was induced in weight-matched 7- to 8-week-old mice by three intraperitoneal injections of STZ (Sigma, St. Louis, MO) (133 mg/kg body wt) dissolved in 10 mmol/l Na citrate, pH 5.5. Control mice received injections with buffer alone. STZ or citrate buffer was administered at three time points occurring at 48-h intervals during the first week. Mice with blood glucose in the range of 250–400 mg/dl were divided into the following four subgroups: *1*) tumstatin treatment for 2 weeks, *2*) vehicle buffer treatment for 2 weeks, *3*) tumstatin treatment for 3 weeks, and *4*) vehicle buffer treatment for 3 weeks ($n = 5$ for each subgroup). Mice of groups 1 and 3 received daily intraperitoneal injection of tumstatin-peptide (T8-peptide) at the dosage of 1 mg/kg body wt, and mice of groups 2 and 4 received vehicle buffer (PBS). Blood glucose levels and urine samples were monitored every week and when needed, and diabetic mice were given supportive insulin treatment (Ultratard; Novo Nordisk) (1 unit/kg body wt twice a week) to prevent ketosis without significantly affecting blood glucose levels. No mice died during the experimental period. At the end of each of the experimental periods, individual 24-h urine sample collections were performed and body weight measured. Nonfasting blood samples were drawn from the retro-orbital venous plexus using heparinized capillary tubes under anesthesia. Kidney weights were measured just after the mice were killed. Tumstatin peptide (amino acid sequence: H-KQRFTTMPFLFCNVNDVCNFASRNDYS-OH) (27) was synthesized and purified by high-performance liquid chromatography (Kurabou, Osaka, Japan; and Multiple Peptide Systems, San Diego, CA) and characterized as previously described (27). Tumstatin peptide, with its purity higher than 96%, was used and dissolved in PBS to be used for the animal experiments. The dosage of tumstatin peptide used in the present study was determined according to previous studies using the tumstatin-derived tum-1 or tum-5 domain in the experimental mouse tumor model in vivo (25,27).

Blood and urine examination. Blood glucose was measured in tail-vein blood, and urine was tested for ketone bodies and glucose by SRL (Okayama, Japan). Serum and urinary creatinine levels were measured by the enzymatic colorimetric method as described (30,31). Urinary albumin concentration was measured by nephelometry (Organon Teknika-Cappel, Durham, NC) using anti-mouse albumin antibody (ICN Pharmaceuticals, Aurora, OH) as previously described (31). Results were normalized to the urinary creatinine levels and expressed as urinary albumin–to–creatinine ratio (UACR). The creatinine clearance (Ccr) was calculated and expressed as milliliters per minute.

Histological analysis. At 2 or 3 weeks after the initiation of treatment, kidneys were removed, fixed in 10% buffered formalin, and embedded in paraffin. Sections (3 μm) were stained with periodic acid-Schiff (PAS) for light microscopic observation. Mean glomerular tuft volume (G_V) was determined from the mean glomerular cross-sectional tuft area (G_A) as described previously (32). Thirty glomeruli from each cortical area were observed, and images were taken and analyzed by using National Institute of Health (NIH) Image software to determine the mean G_A. G_V was calculated as $G_V = \beta/k \times (G_A)^{3/2}$, with $\beta = 1.38$, the shape coefficient for spheres, and $k = 1.1$, a size distribution coefficient (32). More than 30 glomerular cross-sections were observed by two investigators and averaged to determine glomerular cell number and capillary number.

Immunohistochemistry. Immunohistochemistry was performed using frozen or formalin-fixed, paraffin-embedded sections as previously described (26,33). For immunohistochemistry of CD31, paraffin-embedded sections (4 μm) were dewaxed and rehydrated. Endogenous peroxidase was quenched with 3% H_2O_2 for 30 min, and sections were blocked with 10% normal goat serum (Sigma). Sections were incubated with rat anti-mouse CD31 monoclonal antibody (Pharmingen, San Diego, CA) overnight at 4°C. Sections were then washed and incubated with secondary anti-rat IgG antibody, and immunoperoxidase staining was carried out using the Vectastain ABC Elite reagent kit (Vector Labs, Burlingame, CA) as previously described (33,34). Diamino-benzidine was used as a chromogen. All slides were counterstained with hematoxylin. Normal rat IgG was used as a negative control. The number of CD31-positive glomerular capillaries was determined by observing >20 glomeruli from each section.

Glomerular accumulation of monocyte/macrophage was determined by immunohistochemistry using rat anti-mouse F4/80 antibody (Serotec, Oxford, U.K.). Frozen sections were fixed in acetone and subjected to immunoperoxidase staining using the Vectastain ABC Elite reagent kit as previously described (33). Diamino-benzidine was used as a chromogen. The number of F4/80-positive cells was determined by observing >20 glomeruli from each section.

Immunofluorescence staining for type IV collagen or nephrin was performed using frozen kidney sections. Four-micrometer sections were fixed in acetone, blocked with 10% goat serum, and incubated overnight with polyclonal rabbit anti-mouse type IV collagen antibody (Chemicon International, Temecula, CA) or polyclonal guinea pig anti-nephrin antibody (Progen, Heidelberg, Germany). Then, sections were stained with fluorescein isothiocyanate– or rhodamine–conjugated anti-rabbit or guinea pig IgG secondary antibodies for 30 min at room temperature. After washing in PBS, sections were observed by a confocal laser fluorescence microscope (LSM-510; Carl Zeiss, Jena, Germany). The immunoreactivity of type IV collagen was quantified as follows: color images were obtained as TIF files by LSM-510. The brightness of each image file was uniformly enhanced by Photoshop software (Adobe Systems, San Jose, CA), followed by analysis using NIH Image. Image files (TIFF) were inverted and opened in gray-scale mode. Type IV collagen index was calculated using the following formula: {[X (density) × positive area (μm^2)]/glomerular total area (μm^2)}, where the staining density is indicated by a number from 0 to 256 in gray scale.

RNA extraction and quantitative real-time RT-PCR. Kidneys from each mouse were homogenized, and total RNA was extracted using RNeasy Midi Kit (Qiagen, Chatsworth, CA) and stored at −80°C until use. Total RNA was subjected to RT with poly-d (T) primers and reverse transcriptase (RTG T-Primed First-Strand kit; Amersham Pharmacia Biotech, Piscataway, NJ). Quantitative real-time RT-PCR was used to quantify the amounts of nephrin mRNA. cDNA was diluted 1:5 with autoclaved deionized water, and 5 μl of the diluted cDNA was added to Lightcycler-Mastermix, 0.5 μmol/l specific primer, 3 mmol/l $MgCl_2$, and 2 μl Master SYBR Green (Roche Diagnostics, Mannheim, Germany). This reaction mixture was filled up to a final volume of 20 μl with

TABLE 1
Body weight and blood glucose concentration

	Body weight (g)	Blood glucose (mmol/l)
Nondiabetic	19.1 ± 0.7*	5.7 ± 0.6*
2 weeks diabetic (vehicle treated)	16.4 ± 1.7	20.4 ± 8.6
2 weeks diabetic (tumstatin treated)	17.1 ± 1.3	21.5 ± 4.4
3 weeks diabetic (vehicle treated)	16.1 ± 0.7	22.6 ± 4.1
3 weeks diabetic (tumstatin treated)	16.3 ± 0.3	22.1 ± 2.7

Data are means ± SE. *$P < 0.01$ vs. diabetic animals. $n = 5$–6 in each group.

water. PCR was carried out in a real-time PCR cycler (Lightcycler; Roche Diagnostics). The program was optimized and performed finally as denaturation at 95°C for 10 min followed by 40 cycles of amplification (95°C for 10 s, 65°C for 10 s, and 72°C for 10 s). The temperature ramp rate was 20°C per s. At the end of each extension step, the fluorescence was measured to quantitate the PCR products. After completion of the PCR, the melting curve of the product was measured by temperature gradient from 65 to 95°C at 0.2°C per s with continuous fluorescence monitoring to produce a melting profile of the primers. The amount of PCR products was normalized with glyceraldehyde-3-phosphate dehydrogenase (GAPDH) to determine the relative expression ratio for nephrin mRNA in relation to GAPDH mRNA. The following oligonucleotide primers specific for mouse nephrin and GAPDH were used: nephrin, 5′-ATCTCCAAGACCCCAGGTACACA-3′ (forward) and 5′-AGGGTCAGGACGGCTGA T-3′ (reverse); and GAPDH, forward 5′-ATGGT GAAGGTCGGTGTG-3′ and reverse 5′-ACCAGTGGATGCAGGGAT-3′. Four independent experiments were performed.

Immunoblot. Immunoblot was performed as previously described (29). Briefly, kidneys were homogenized in radioimmunoprecipitation assay (RIPA) buffer (30 μl 2.2 mg/ml aprotinin, 10 μl 10 μg/ml phenylmethylsulfonyl fluoride, and 10 μl 100 mmol/l sodium orthovanadate per 1 ml RIPA buffer) at 4°C. After centrifugation at 14,000 rpm for 30 min at 4°C, supernatant was collected and stored at −80°C until use. Total protein concentration was determined by using the DC-protein determination system (Bio-Rad) using BSA as a standard. Samples were processed for SDS-PAGE, and proteins were electrotransferred onto nitrocellulose membrane (Hybond-ECL; Amersham). The membranes were blocked with 5% nonfat dry milk in 1× TBS (0.1% Tween-20) for 1 h, incubated overnight with polyclonal rabbit anti-mouse Ang-1, Ang-2 (Alpha diagnostics, San Antonio, TX), anti-VEGF, flk-1, and Tie-2 (SantaCruz) antibodies at 4°C. After incubation with horseradish peroxidase–labeled secondary antibodies for 1 h, signals were detected with an enhanced chemiluminescence system (Amersham). Membranes were reprobed with rabbit polyclonal anti-actin antibodies (Bio-Rad) to serve as controls for equal loading. The density of each band was determined using NIH Image software and expressed as a value relative to the density of the corresponding band obtained from the actin immunoblot.

Statistical analysis. All values are expressed as means ± SE. ANOVA with a one-tailed Student's t test was used to identify significant differences in multiple comparisons. A level of $P < 0.05$ was considered statistically significant.

RESULTS

Changes in blood glucose, body weight, and kidney weight/body weight. Administration of tumstatin peptide did not change plasma glucose concentrations as compared with diabetic mice treated with vehicle buffer after 2 or 3 weeks of treatment (Table 1). Body weight was significantly lower in all of the diabetic groups as compared with the nondiabetic animals. There was no significant difference in body weight between diabetic mice treated with tumstatin peptide and diabetic animals treated with vehicle buffer. Diabetic animals exhibited significantly greater kidney weight–to–body weight ratio as compared with nondiabetic mice (Fig. 1*A*). Treatment with tumstatin peptide for 2 or 3 weeks resulted in significantly decreased kidney weight–to–body weight ratio as compared with vehicle-treated diabetic mice (Fig. 1*A*).

Changes in serum creatinine, Ccr, and urinary albumin excretion. Serum creatinine levels did not significantly differ among the experimental groups (nondiabetic control 0.100 ± 0.004 mg/dl at 2 weeks, 0.093 ± 0.006 vs. 0.098 ± 0.005 mg/dl at 3 weeks; 0.097 ± 0.007 vs. 0.097 ±

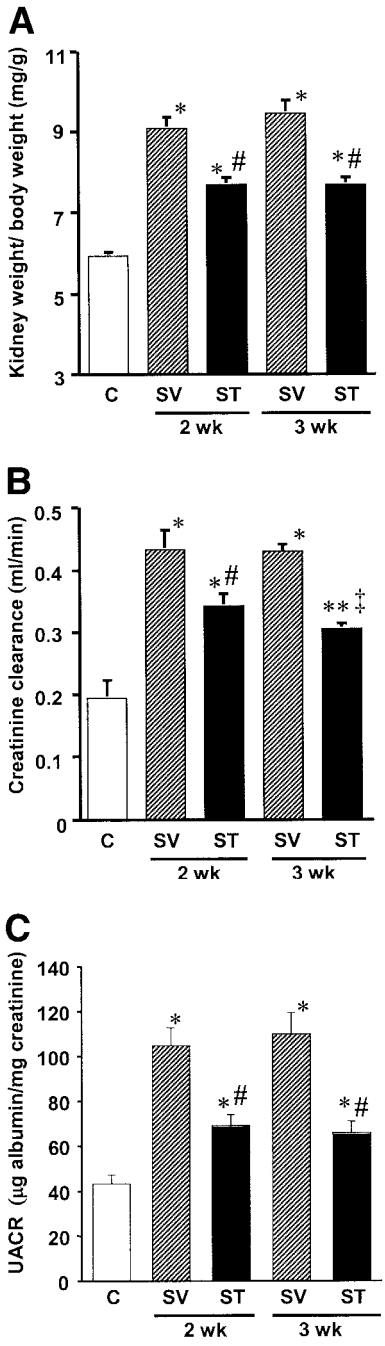

FIG. 1. *A*: Increase in kidney weight/body weight induced by STZ was diminished after tumstatin treatment for 2 or 3 weeks. Kidney weight relative to body weight was determined before termination of the experiments. *$P < 0.01$ vs. C; #$P < 0.02$ vs. SV at the same time points. *B*: Increase in Ccr induced by STZ was partially suppressed by tumstatin treatment. *$P < 0.01$ vs. C; ‡$P < 0.05$ vs. C; #$P < 0.02$ vs. SV at the same time points. **$P < 0.01$ vs. SV at the same time points. *C*: Increase in UACR induced by STZ was partially suppressed by tumstatin treatment. *$P < 0.01$ vs. C; #$P < 0.01$ vs. SV at the same time points. $n = 5$ for each group. C, nondiabetic control; SV, diabetic mice treated with vehicle buffer; ST, diabetic mice treated with tumstatin peptide. Each column consists of means ± SE.

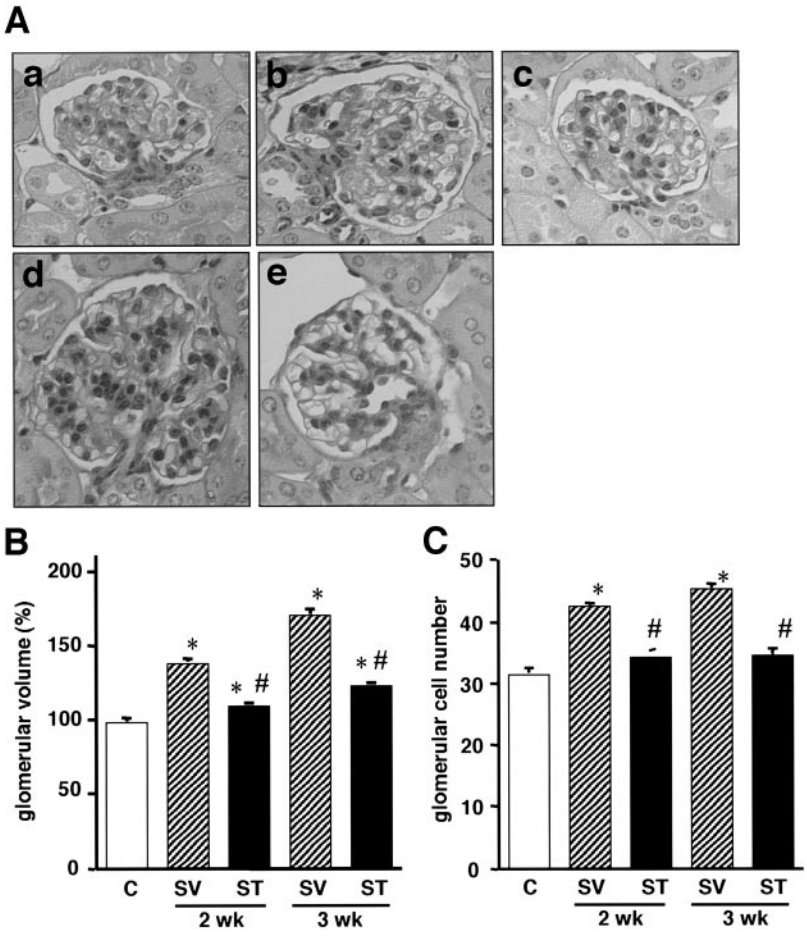

FIG. 2. ***A*****: Representative light microscopic appearance of glomeruli (PAS staining, 400× original magnification) for nondiabetic control mice (*a*), diabetic mice treated with vehicle buffer for 2 weeks (*b*), diabetic mice treated with tumstatin peptide for 2 weeks (*c*), diabetic mice treated with vehicle buffer for 3 weeks (*d*), and diabetic mice treated with tumstatin peptide for 3 weeks (*e*) (histological parameters).** ***B*****: Increase in glomerular volume induced by STZ was diminished after tumstatin treatment for 2 or 3 weeks. Glomerular volume was determined as described in RESEARCH DESIGN AND METHODS. ****P* **< 0.01 vs. C; #***P* **< 0.01 vs. SV at the same time points.** ***C*****: Increase in total glomerular cell number in diabetic mice was suppressed by tumstatin treatment. ****P* **< 0.0001 vs. C; #***P* **< 0.0001 vs. SV at the same time points;** ***n*** **= 5 for each group. C, nondiabetic control; SV, diabetic mice treated with vehicle buffer; ST, diabetic mice treated with tumstatin peptide. Each column consists of means ± SE.**

0.008 mg/dl for tumstatin peptide versus vehicle buffer, respectively). To evaluate the effect of tumstatin peptide on preventing hyperfiltration induced by STZ, we measured Ccr and urinary albumin excretion (Fig. 1*B* and *C*). Although diabetic mice treated with vehicle buffer showed a marked elevation of Ccr and UACR, tumstatin peptide treatment significantly suppressed STZ-induced increases of Ccr and UACR (Ccr of nondiabetic mice 0.20 ± 0.03; Ccr of diabetic mice at 2 weeks 0.35 ± 0.02 vs. 0.47 ± 0.03 ml/min; Ccr of diabetic mice at 3 weeks 0.30 ± 0.01 vs. 0.46 ± 0.01 ml/min; UACR of nondiabetic mice 43.2 ± 4.1; UACR of diabetic mice at 2 weeks 68.9 ± 5.0 vs. 104.6 ± 8.1 μg albumin/mg creatinine; UACR of diabetic mice at 3 weeks 65.6 ± 5.3 vs. 109.6 ± 9.7 μg albumin/mg creatinine for tumstatin peptide versus vehicle buffer, respectively). The development of glomerular hyperfiltration in the diabetic mice was partially but significantly prevented by treatment with tumstatin peptide.

Histology and morphometric analysis. Histological examination of the kidneys revealed glomerular hypertrophy and expansion of mesangial area induced by STZ (Fig. 2). After 2 weeks of treatment by tumstatin peptide, glomerular hypertrophy and mesangial expansion induced by STZ was inhibited in contrast to vehicle buffer–treated animals. At 2 and 3 weeks after starting treatment, tumstatin peptide dramatically inhibited glomerular hypertrophy as compared with the vehicle buffer group. Morphometric analysis (Fig. 2*B* and *C*) revealed that tumstatin peptide significantly inhibited the increase of glomerular volume and cell number as compared with vehicle buffer treatment (glomerular volume at 2 weeks 110.5 ± 2.3 vs. 139.9 ± 3.2%, glomerular volume at 3 weeks 124.5 ± 2.5 vs. 172.7 ± 5.0%, cell number at 2 weeks 34.1 ± 0.6 vs. 42.4 ± 1.5, cell number at 3 weeks 34.5 ± 1.0 vs. 45.3 ± 0.8 for tumstatin peptide versus vehicle buffer, respectively). These results indicate that STZ-induced histological changes associated with glomerular hypertrophy were significantly diminished after tumstatin treatment.

Immunohistochemical analysis of glomerular type IV collagen expression. To further evaluate the therapeutic effect of tumstatin peptide in early diabetic nephropathy, the expression level of type IV collagen was examined by immunofluorescence staining (Fig. 3*A*–*F*). The amount of type IV collagen in glomeruli was increased in the diabetic group (Fig. 3*B*) as compared with nondiabetic mice (Fig. 3*A*). Enhanced immunoreactivity in diabetic mice was observed mainly in glomerular basement membrane and mesangial area. Treatment with tumstatin peptide (3 weeks) decreased the accumulation of type IV collagen induced by STZ (Fig. 3*C*). Quantitative analysis revealed significant inhibitory effect of tumstatin peptide on glomerular accumulation of type IV collagen induced by STZ as compared with vehicle buffer treatment (Fig. 3*D*–*G*).

Immunohistochemical analysis of glomerular CD31 expression. We next examined the expression of endothelial cell marker CD31 in glomeruli. In nondiabetic mice, CD31 was detected in glomerular capillaries (Fig. 4*A*), and increased expression mainly localized to glomerular endothelial cells was observed in control diabetic mice (Fig. 4*B*). Treatment with tumstatin peptide (3 weeks) markedly

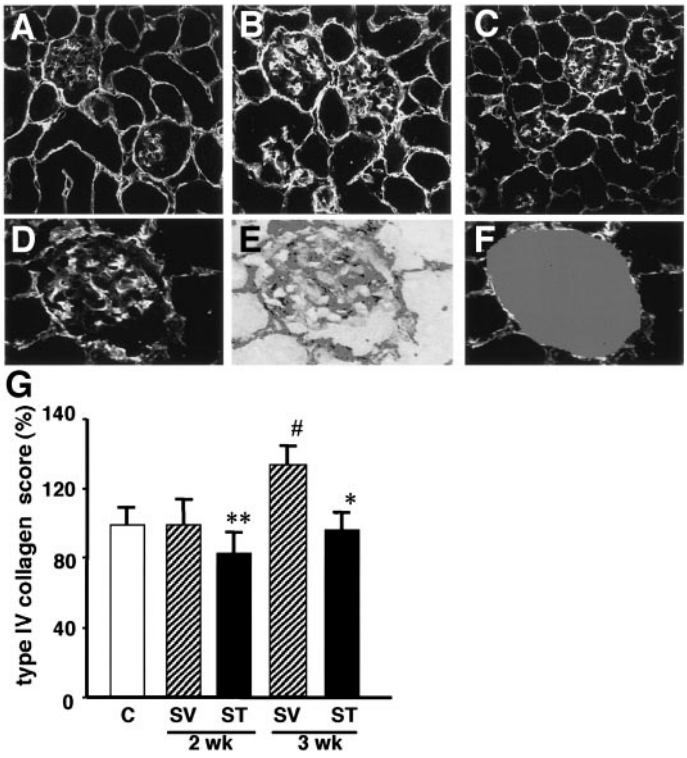

FIG. 3. Glomerular accumulation of type IV collagen was assessed by indirect immunofluorescence method as described in RESEARCH DESIGN AND METHODS for nondiabetic control mice (*A*), diabetic mice treated with vehicle buffer for 3 weeks (*B*), and diabetic mice treated with tumstatin peptide for 3 weeks (*C*). *D*: Image of glomerulus by fluorescent photomicrograph. *E*: Inverted image of the same glomerulus showing the immunoreactivity in red color. *F*: The assessed glomerular area expressed in gray color. *A–C* ×200 and *D–F* ×400 original magnification. *G*: The amount of immunoreactive type IV collagen in glomeruli relative to nondiabetic control group determined by NIH Image is shown; $n = 5$ for each group. C, nondiabetic control; SV, diabetic mice treated with vehicle buffer; ST, diabetic mice treated with tumstatin peptide. *$P < 0.0001$ vs. SV at the same time point; **$P < 0.05$ vs. SV at the same time point; #$P < 0.001$ vs. C, SV, or ST at 2 weeks. Each column consists of means ± SE.

decreased the expression of CD31 in glomeruli (Fig. 4*C*). The number of CD31-expressing glomerular capillaries was significantly increased in diabetic animals, but the STZ-induced increase in glomerular capillary number was significantly suppressed by tumstatin peptide (Fig. 4*D*). These results demonstrate that tumstatin treatment resulted in the inhibition of increase in glomerular CD31-positive endothelial area induced by hyperglycemia possibly via its potent anti-angiogenic efficacy.

Immunohistochemical analysis of monocyte/macrophage accumulation. We next examined the expression of monocyte/macrophage surface marker F4/80 in glomeruli. In diabetic mice, the number of F4/80-positive cells was significantly increased as compared with nondiabetic controls (Fig. 5). Treatment with tumstatin peptide (3 weeks) markedly decreased the accumulation of monocyte/macrophage in glomeruli, suggesting the anti-inflammatory action of tumstatin in this model.

Expression of VEGF, Ang-1, and Ang-2 protein and receptors. The effect of tumstatin peptide on the expression of angiogenesis-associated factors VEGF, Ang-1, and Ang-2 and corresponding receptors flk-1 and Tie-2 in the renal cortex was studied by immunoblot. The level of VEGF and flk-1 was significantly increased in diabetic mice, which is inconsistent with previous reports using STZ-induced diabetic rats (9). Tumstatin treatment significantly suppressed the STZ-induced increase of VEGF and flk-1 (Fig. 6*A*, *B*, *E*, and *F*). The expression of Ang-1 was detected in undiseased mice, not significantly altered by STZ, and tumstatin treatment did not affect on the expression of Ang-1 (Fig. 6*A* and *C*). In contrast, the protein level of Ang-2, an endogenous antagonist of Ang-1 (tie-2 ligand) involved in the induction of sprouting angiogenesis, was increased in diabetic mice as compared with undiseased mice (Fig. 6*A* and *D*). Treatment with tumstatin peptide resulted in marked reduction of Ang-2 in diabetic mice as compared with vehicle-treated mice. The level of Tie-2 was mildly decreased in diabetic mice as compared with nondiabetic control mice (Fig. 6*E* and *G*). Treatment with tumstatin peptide did not affect on the level of Tie-2 in diabetic mice. These experiments were repeated three times with similar results.

Expression of nephrin mRNA and protein. The mRNA and protein expression of nephrin, a pivotal component protein of slit-diaphragm involved in the regulation of filtration barrier, was assessed by real-time RT-PCR and immunohistochemistry. Diabetic mice exhibited reduced expression of nephrin mRNA. Tumstatin treatment resulted in recovery of nephrin mRNA expression (Fig. 7). Immunohistochemistry revealed the podocyte-specific localization of nephrin in undiseased mice and decreased as well as altered the expression pattern observed mainly in the central aspect of glomeruli rather than the peripheral pattern in diabetic mice (Fig. 7). Tumstatin treatment resulted in the restoration of nephrin expression with dominant localization along the glomerular capillary area (Fig. 7). These results suggest a supportive role of tumstatin in maintaining nephrin and thus the glomerular filtration barrier, leading to the suppression of albuminuria induced by STZ.

DISCUSSION

The major microvascular complications of diabetes are composed of diabetic retinopathy, neuropathy, and nephropathy. Among these three complications, patients with diabetic nephropathy require careful management, considering the cardiovascular morbidity and mortality associated with this complication.

Angiogenesis, the formation of new blood vessels from preexisting ones, are composed of several steps, *1*) the degradation of vascular basement membrane matrix by protease, *2*) migration and proliferation of endothelial cells, *3*) endothelial tube formation, *4*) recruitment and attachment of mesenchymal cells to the tube, and *5*) maturation of blood vessels (35). Angiogenic growth factor VEGF induces the activation of matrix-degrading protease represented by matrix metalloprotease, migration, and proliferation of endothelial cells (36). Another angiogenesis-associated factor Ang-1 is involved in the attachment of mesenchymal cells to endothelial tube and differentiation to "pericytes," resulting in mature, "nonleaky" blood vessels (13). Ang-1 binds to the tyrosine kinase receptor Tie-2 and promotes the firm attachment of pericytes (13). Ang-2 is the natural antagonist of Ang-1 and loosens the attachment of pericytes, resulting in promoting sprouting angiogenesis in the presence of VEGF (14).

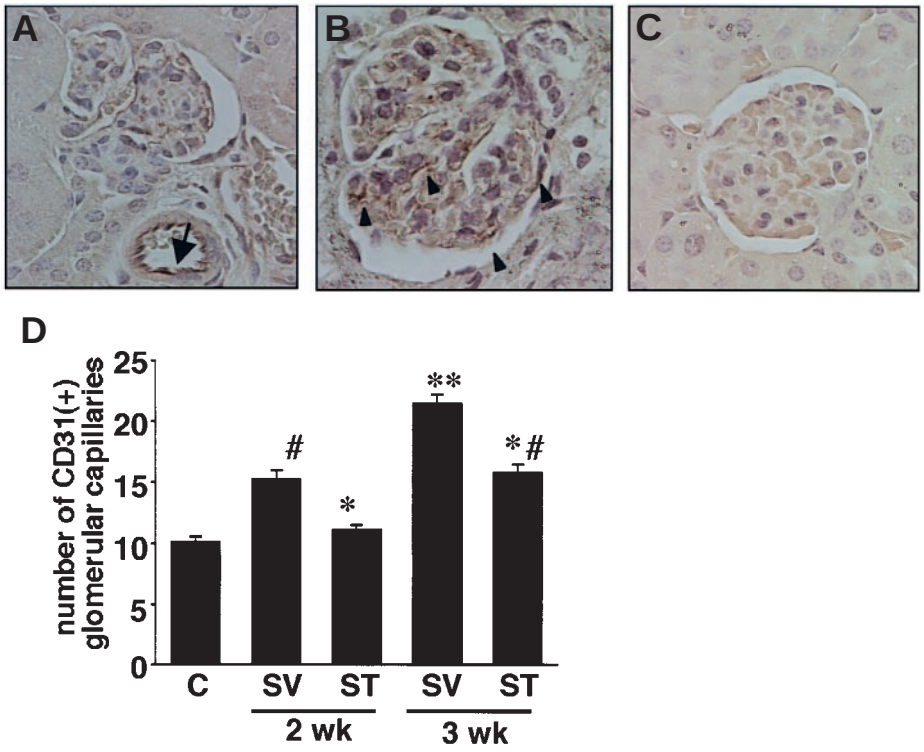

FIG. 4. Immunohistochemistry of CD31, an endothelial cell marker. Distribution of CD31 was determined as described in RESEARCH DESIGN AND METHODS by indirect immunohistochemistry in nondiabetic control mice (*A*), diabetic mice treated with vehicle buffer for 3 weeks (*B*), and diabetic mice treated with tumstatin peptide for 3 weeks (*C*). CD31 was observed in glomerular endothelium (arrowheads) and in endothelial cells of extraglomerular blood vessels (arrow). Representative light microscopic appearance of glomerulus is shown (400× original magnification). *D*: Glomerular CD31-positive capillary number was determined as described in RESEARCH DESIGN AND METHODS. Increase in CD31(+) glomerular capillary number was significantly suppressed after tumstatin treatment; $n = 5$ for each group. C, Nondiabetic control; SV, diabetic mice treated with vehicle buffer; ST, diabetic mice treated with tumstatin peptide. *$P < 0.001$ vs. SV at the same time points; #$P < 0.01$ vs. C; **$P < 0.001$ vs. ST or SV at 2 weeks or C. Each column consists of means ± SE.

The involvement of VEGF in progressing diabetic nephropathy is demonstrated in a number of previous reports suggesting the therapeutic potential of the inhibition of VEGF signaling (9–12). To date, the involvement of Ang-1, Ang-2, and Tie-2 in the process of diabetic nephropathy is not studied extensively. In contrast, the involvement of these factors has been demonstrated in the setting of diabetic retinopathy. Increased expression of VEGF (37) and therapeutic efficacy of Ang-1 associated with anti-inflammatory bioactivities have been reported in diabetic retinopathy (38). The morphological phenomenon observed in diabetic nephropathy (capillary elongation and increased glomerular capillary number) suggests the involvement of the angiogenic process in analogy with diabetic retinopathy, thus implicating the possible involvement of Ang-1 and Ang-2 in addition to VEGF in the progression of diabetic nephropathy.

Tumstatin, an endogenous inhibitor of tumor and angiogenesis, inhibits cell proliferation, specifically in endothelial cells (25–29,39). Tumstatin also inhibits in vivo neo-

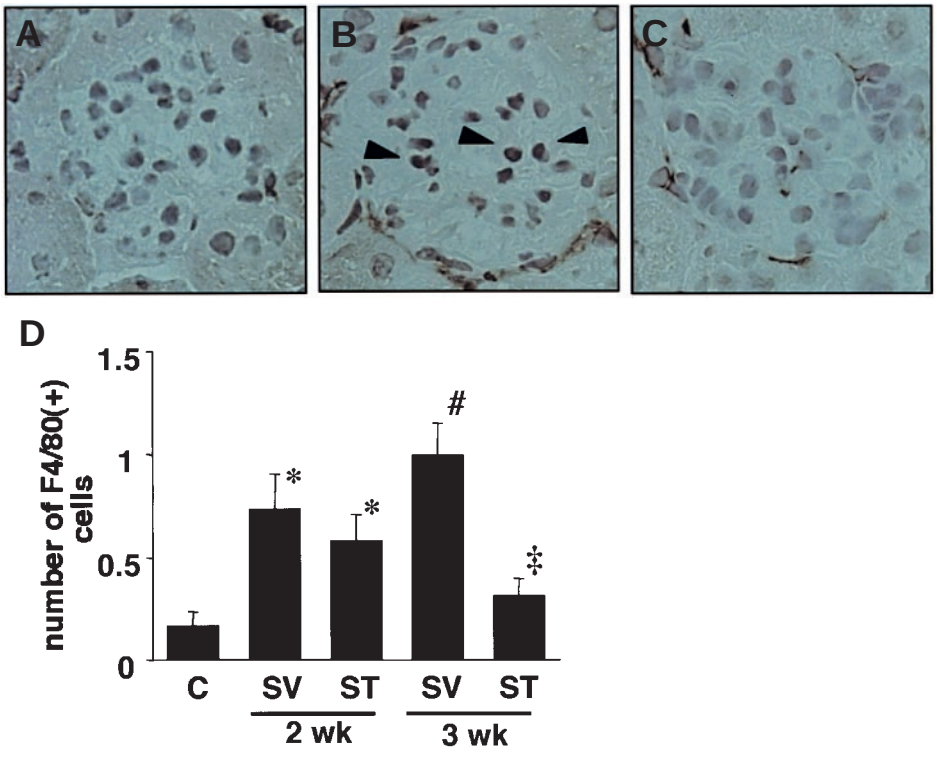

FIG. 5. Immunohistochemistry of F4/80(+) monocyte/macrophage. Distribution of F4/80(+) cells was determined by indirect immunohistochemistry for nondiabetic control mice (*A*), diabetic mice treated with vehicle buffer for 3 weeks (*B*), and diabetic mice treated with tumstatin peptide for 3 weeks (*C*). F4/80-positive macrophages were observed in diabetic mice (arrowheads) and in tumstatin-treated diabetic mice to a lesser extent. Representative light microscopic appearance of glomerulus is shown (400× original magnification). *D*: The number of glomerular F4/80-positive monocyte/macrophage is shown. Increase in F4/80(+) monocyte/macrophage number was significantly suppressed after tumstatin treatment; $n = 5$ for each group. C, Nondiabetic control; SV, diabetic mice treated with vehicle buffer; ST, diabetic mice treated with tumstatin peptide. *$P < 0.01$ vs. C; #$P < 0.0001$ vs. C; ‡$P < 0.001$ SV at the same time point. Each column consists of means ± SE.

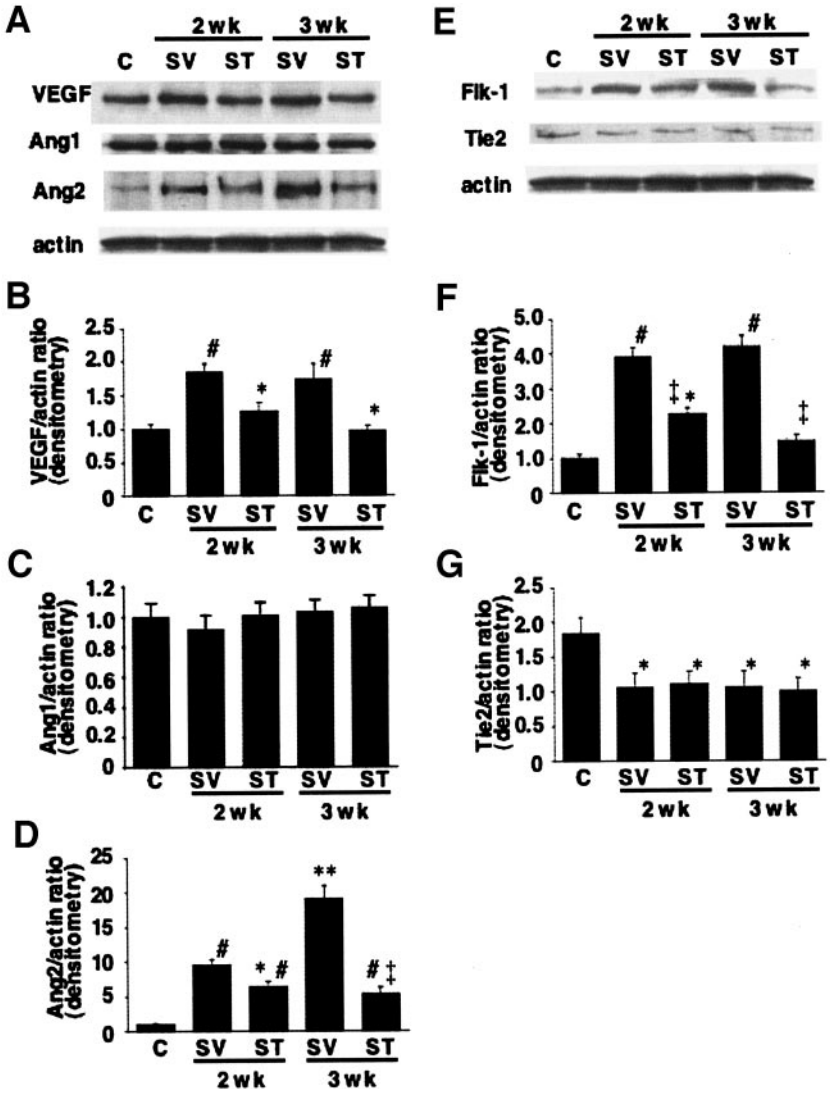

FIG. 6. Immunoblot analysis. *A*: Immunoblots for VEGF, Ang-1, Ang-2, and actin are shown. In each lane, 30 μg protein obtained from kidney cortex was loaded. Each band was scanned and subjected to densitometry. *B*: Intensities of VEGF protein relative to actin are shown. **P* < 0.05 vs. SV at the same time points; #*P* < 0.05 vs. C. *C*: Intensities of Ang-1 protein relative to actin are shown. *D*: Intensities of Ang-2 protein relative to actin are shown. **P* < 0.05 vs. SV at the same time point; ‡*P* < 0.01 SV at the same time point; #*P* < 0.05 vs. C; ***P* < 0.01 vs. C. *E*: Immunoblots for flk-1, Tie-2, and actin are shown. In each lane, 30 μg protein obtained from kidney cortex was loaded. Each band was scanned and subjected to densitometry. *F*: Intensities of flk-1 protein relative to actin are shown. **P* < 0.05 vs. C. #*P* < 0.01 vs. C; ‡*P* < 0.05 vs. SV at the same time points. *G*: Intensities of Tie-2 protein relative to actin are shown. **P* < 0.05 vs. C. C, Nondiabetic control; SV, diabetic mice treated with vehicle buffer; ST, diabetic mice treated with tumstatin peptide. *n* = 4 for each group. Each column consists of mean ± SE.

vascularization induced by VEGF, suggesting its potential therapeutic efficacy in diabetic nephropathy, since upregulation of VEGF and VEGF receptors have been reported in diabetic nephropathy (9,10). In the present study, we used a diabetic nephropathy mouse model induced by STZ and examined the therapeutic efficacy of tumstatin peptide.

In diabetic mice, characteristic changes in early diabetic nephropathy, such as increased urinary albumin excretion, glomerular hypertrophy, glomerular hyperfiltration as evidenced by increased Ccr and increase in kidney weight relative to body weight, were observed. In contrast, inhibitory effects on these early abnormalities in diabetic nephropathy were observed in diabetic mice treated with tumstatin peptide. The increase in glomerular cell number was significantly suppressed after tumstatin treatment. It is well known that renal glomeruli are composed of three types of resident cells: endothelial, mesangial, and epithelial cells (podocytes). Although we could not determine exactly which cell type has contributed to the decreased glomerular cell number in animals treated with tumstatin peptide, we speculate that it was reflected by the decrease in endothelial cell number, at least in part, considering the decreased CD31-positive glomerular capillary number. We speculate that this effect was mediated via the potent antiangiogenic efficacy of tumstatin peptide. In addition, increased accumulation of monocyte/macrophage in glomeruli had been reported in diabetic nephropathy in human and animal models (31). Considering the effect of VEGF in promoting vascular permeability, it is possible that increased monocyte/macrophage accumulation in diabetic nephropathy may also be partially mediated via stimulation of VEGF. Since tumstatin potently inhibits VEGF-induced angiogenic action, we speculate that the inhibitory effect of tumstatin peptide on the recruitment of monocyte/macrophage was mediated, at least in part, via interference in VEGF signal, leading to decreased vascular permeability.

Next, we observed the inhibitory effect of tumstatin peptide on the accumulation of type IV collagen in glomeruli in diabetic mice. Since the NC1 domain of type IV collagen is speculated to play a crucial role in the assembly of type IV collagen to form trimers (24), it is suggested that tumstatin inhibited the accumulation of type IV collagen by modulating the assembly of collagen chains. In general, trimers consisting of α3, α4, and α5 chains of type IV collagen are the dominant component of glomerular basement membrane (40). Considering that tumstatin is derived from α3(IV) chain, tumstatin may have suppressed

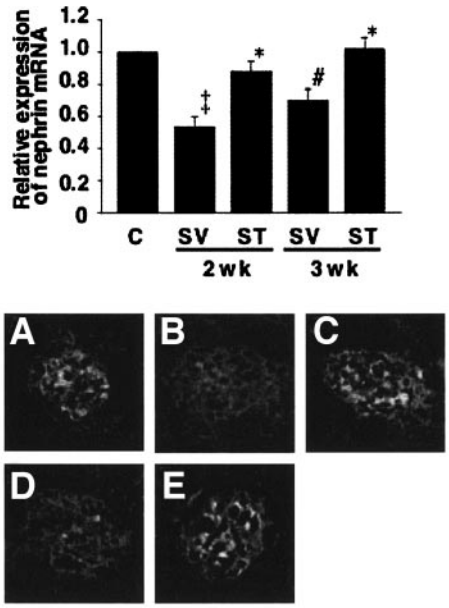

FIG. 7. ***Upper panel*****: Expression of nephrin mRNA detected by real-time RT-PCR. Total RNA was extracted from kidney cortex and subjected to the examination using quantitative real-time RT-PCR as described in RESEARCH DESIGN AND METHODS. The amount of nephrin mRNA relative to GAPDH mRNA is shown. Results were expressed relative to nondiabetic control mice that were arbitrarily assigned a value of 1.0. C, nondiabetic control; SV, diabetic mice treated with vehicle buffer; ST, diabetic mice treated with tumstatin peptide; $n = 4$ for each group. *$P < 0.05$ vs. SV at the same time points; #$P < 0.05$ vs. C; ‡$P < 0.01$ vs. C. Each column consists of mean ± SE.** ***Lower panels*****: Immunofluorescent staining of nephrin in kidneys. Representative fluorescent photomicrographs of nondiabetic control (*A*), diabetic mice treated with vehicle buffer for 2 weeks (*B*), diabetic mice treated with tumstatin peptide for 2 weeks (*C*), diabetic mice treated with vehicle buffer for 3 weeks (*D*), and diabetic mice treated with tumstatin peptide for 3 weeks (*E*) (original magnification ×400). Note the capillary distribution pattern of nephrin in *A*, *C*, and *E*. The intenstity of nephrin is diminished exhibiting central localization pattern in *B* and *D*.**

excess assembly of trimers consisting of α3, α4, and α5(IV) chains, thus leading to reduced thickening of glomerular basement membranes induced by STZ. The pivotal role of TGF-β1 in renal fibrosis has been well characterized (41). We could not observe evident differences in the expression level of TGF-β1 between tumstatin- and vehicle-treated diabetic mice (immunohistochemistry, data not shown), suggesting that the therapeutic effect of tumstatin on the accumulation of glomerular type IV collagen was mediated via altered matrix assembly rather than the inhibition of TGF-β1.

Then, the effect of tumstatin-peptide on angiogenesis-associated factors was examined. The level of VEGF and flk-1 was markedly increased in the kidney of diabetic mice, inconsistent with previous studies (9–12). In contrast, tumstatin treatment significantly suppressed the increase of VEGF as well as flk-1 in kidneys of diabetic mice. The therapeutic effect of tumstatin peptide in early diabetic nephropathy may be attributed at least in part to the inhibition of the VEGF pathway, which is analogous with previous studies using neutralizing anti-VEGF antibodies (11,12). The potential advantages of tumstatin peptide over anti-VEGF antibodies would be that tumstatin-peptide is derived from human endogenous matrix protein, that peptide can be produced feasibly with less cost as compared with antibodies, and that immune responses by antibody production are unlikely. A previous report (42) demonstrated the effect of VEGF to augment protein synthesis and hypertrophy in mouse renal proximal tubular epithelial cells in a PI 3-kinase– and Akt-dependent manner. The effect of tumstatin peptide in suppressing the increase of VEGF and flk-1 in diabetic mice might have lead to decreased protein synthesis and reduced hypertrophy in tubular epithelial cells, thus resulting in the reduction in the kidney weight–to–body weight ratio. Although the expression of Ang-1 was not altered, the expression of Ang-2 was markedly increased in diabetic mice. Tumstatin treatment did not affect Ang-1 level but significantly decreased the expression of Ang-2 close to the level of nondiabetic mice. The level of Tie-2 was mildly decreased in diabetic mice as compared with nondiabetic mice, and tumstatin peptide did not alter the level of Tie-2. These results suggest the dominant involvement of changes in the level of ligand protein (Ang-1/2) rather than changes in the level of receptor (Tie-2) regarding the effect of tumstatin peptide in this model. The marked increase of Ang-2 over Ang-1 in diabetic mice suggests the proangiogenic milieu considering simultaneous upregulation of VEGF and unstable condition of capillaries possibly associated with inflammatory response, such as monocyte recruitment as evidenced by F4/80 immunostaining. These results suggest the biological function of tumstatin peptide as an antiangiogenic peptide in a diabetic nephropathy model, similar to its efficacy reported on tumor models (25,26).

Nephrin, the first true functional molecule of the interpodocyte filtration slit diaphragm (43), has been discovered from genetic studies of patients with the congenital nephritic syndrome of the Finnish type, showing that mutations in the gene coding nephrin (NPHS1) are associated with massive proteinuria (16). A correlation between altered expression of nephrin and proteinuria has been shown in various experimental models of renal disorders. Altered distribution as well as reduced expression of nephrin in glomeruli has been demonstrated in patients with nephrotic syndrome (44). In the setting of diabetic nephropathy, recent studies have shown the altered expression pattern of nephrin (17,19,45). Reduction in both mRNA and protein expression of nephrin was associated with proteinuria in diabetic spontaneously hypertensive rats (45). In STZ-induced rat diabetes models and in NOD mice, redistribution of nephrin from a glomerular epithelial cell pattern to a more central glomerular area, increased nephrin mRNA expression, and loss of nephrin protein into urine were observed (17). These changes were attributed to the increase in the variant form of nephrin protein lacking the transmembrane spanning domain due to the alternatively spliced nephrin mRNA (46). In human type 1 and type 2 diabetic nephropathy, redistribution and reduced expression of nephrin in glomeruli have been demonstrated (19). In the present study, we observed decreased nephrin mRNA expression in diabetic mice and the recovered expression of nephrin after tumstatin treatment. To date, there are no reports on nephrin gene and protein expression using STZ-induced diabetic mice models. In the present study, we have used PCR primers for nephrin designed to amplify the extracellular domain close to the transmembrane domain (17)

considering the possible influence by alternatively spliced nephrin mRNA. We also examined nephrin mRNA level using distinct pairs of primers designed against the NH_2-terminal domain and obtained similar results (data not shown). The pattern of nephrin protein expression was altered in diabetic mice similar to previous studies with more central localization and less epithelial staining in glomeruli and was recovered after tumstatin treatment. Considering the pivotal role of nephrin in the maintenance of glomerular filtration barrier, the recovery of nephrin after tumstatin treatment might be associated with decreased albuminuria. Although we could not clarify the precise mechanism of action of tumstatin peptide on nephrin that is exclusively expressed on podocytes, the indirect influence of glomerular endothelial cells toward podocytes (possibly mediated via secreted factors or alteration on matrix microenvironment) might be involved. A recent genetic study (47) using mice with podocyte-specific overexpression or deletion of VEGF demonstrated the development of proteinuria and pathological changes in glomerular endothelial cells, suggesting the importance of appropriate level of VEGF in maintaining glomerular filtration barrier. The suggested role of Ang-1 in maintaining glomerular endothelium and regulating the action of VEGF on glomerular permselectivity (48) further supports the importance of the interaction between glomerular endothelial cells and podocytes in maintaining glomerular structures as well as biological functions.

In conclusion, we demonstrated that antiangiogenic tumstatin peptide effectively ameliorated alterations in early diabetic nephropathy induced by STZ. To date, this is the first report showing the efficacy of endogenous antiangiogenic factors in preventing the progression of diabetic nephropathy. These results implicate the therapeutic potential of tumstatin peptide on human diabetic nephropathy, in addition to its potent effect on the treatment of tumor and metastasis.

ACKNOWLEDGMENTS

A portion of this study was supported by a grant-in-aid for Scientific Research from the Ministry of Education, Science and Culture of Japan (to Y.M.) and by a grant-in-aid from the Tokyo Biochemical Research Foundation (to Y.M.). Y.M. is a recipient of the 2001 Research Award from the Okayama Medical Foundation, the 2002 Research Award from the KANAE Foundation for Life & Socio-Medical Science, the 2002 Young Investigator Award from the Japan Society of Cardiovascular Endocrinology and Metabolism, the 2003 Research Award from the Kobayashi Magobei Memorial Foundation for Medical Science, the 2003 Research Award from the Ryobi Teien Memorial Foundation, and the 2004 Research award from the Inamori Foundation.

REFERENCES

1. Ritz E, Rychlik I, Locatelli F, Halimi S: End-stage renal failure in type 2 diabetes: a medical catastrophe of worldwide dimensions. *Am J Kidney Dis* 34:795–808, 1999
2. Osterby R, Parving HH, Nyberg G, Hommel E, Jorgensen HE, Lokkegaard H, Svalander C: A strong correlation between glomerular filtration rate and filtration surface in diabetic nephropathy. *Diabetologia* 31:265–270, 1988
3. Makino H, Yamasaki Y, Haramoto T, Shikata K, Hironaka K, Ota Z, Kanwar YS: Ultrastructural changes of extracellular matrices in diabetic nephropathy revealed by high resolution scanning and immunoelectron microscopy. *Lab Invest* 68:45–55, 1993
4. Makino H, Kashihara N, Sugiyama H, Kanao K, Sekikawa T, Okamoto K, Maeshima Y, Ota Z, Nagai R: Phenotypic modulation of the mesangium reflected by contractile proteins in diabetes. *Diabetes* 45:488–495, 1996
5. Sharma K, Ziyadeh FN: Hyperglycemia and diabetic kidney disease: the case for transforming growth factor-β as a key mediator. *Diabetes* 44: 1139–1146, 1995
6. Flyvbjerg A: Putative pathophysiological role of growth factors and cytokines in experimental diabetic kidney disease. *Diabetologia* 43:1205–1223, 2000
7. Ferrara N: Vascular endothelial growth factor and the regulation of angiogenesis. *Recent Prog Horm Res* 55:15–35, 2000
8. Tilton RG, Chang KC, LeJeune WS, Stephan CC, Brock TA, Williamson JR: Role for nitric oxide in the hyperpermeability and hemodynamic changes induced by intravenous VEGF. *Invest Ophthalmol Vis Sci* 40:689–696, 1999
9. Cooper ME, Vranes D, Youssef S, Stacker SA, Cox AJ, Rizkalla B, Casley DJ, Bach LA, Kelly DJ, Gilbert RE: Increased renal expression of vascular endothelial growth factor (VEGF) and its receptor VEGFR-2 in experimental diabetes. *Diabetes* 48:2229–2239, 1999
10. Tsuchida K, Makita Z, Yamagishi S, Atsumi T, Miyoshi H, Obara S, Ishida M, Ishikawa S, Yasumura K, Koike T: Suppression of transforming growth factor beta and vascular endothelial growth factor in diabetic nephropathy in rats by a novel advanced glycation end product inhibitor, OPB-9195. *Diabetologia* 42:579–588, 1999
11. de Vriese AS, Tilton RG, Elger M, Stephan CC, Kriz W, Lameire NH: Antibodies against vascular endothelial growth factor improve early renal dysfunction in experimental diabetes. *J Am Soc Nephrol* 12:993–1000, 2001
12. Flyvbjerg A, Dagnaes-Hansen F, De Vriese AS, Schrijvers BF, Tilton RG, Rasch R: Amelioration of long-term renal changes in obese type 2 diabetic mice by a neutralizing vascular endothelial growth factor antibody. *Diabetes* 51:3090–3094, 2002
13. Suri C, Jones PF, Patan S, Bartunkova S, Maisonpierre PC, Davis S, Sato TN, Yancopoulos GD: Requisite role of angiopoietin-1, a ligand for the TIE2 receptor, during embryonic angiogenesis. *Cell* 87:1171–1180, 1996
14. Maisonpierre PC, Suri C, Jones PF, Bartunkova S, Wiegand SJ, Radziejewski C, Compton D, McClain J, Aldrich TH, Papadopoulos N, Daly TJ, Davis S, Sato TN, Yancopoulos GD: Angiopoietin-2, a natural antagonist for Tie-2 that disrupts in vivo angiogenesis. *Science* 277:55–60, 1997
15. Woolf AS, Yuan HT: Angiopoietin growth factors and Tie receptor tyrosine kinases in renal vascular development. *Pediatr Nephrol* 16:177–184, 2001
16. Kestila M, Lenkkeri U, Mannikko M, Lamerdin J, McCready P, Putaala H, Ruotsalainen V, Morita T, Nissinen M, Herva R, Kashtan CE, Peltonen L, Holmberg C, Olsen A, Tryggvason K: Positionally cloned gene for a novel glomerular protein–nephrin–is mutated in congenital nephrotic syndrome. *Mol Cell* 1:575–582, 1998
17. Aaltonen P, Luimula P, Astrom E, Palmen T, Gronholm T, Palojoki E, Jaakkola I, Ahola H, Tikkanen I, Holthofer H: Changes in the expression of nephrin gene and protein in experimental diabetic nephropathy. *Lab Invest* 81:1185–1190, 2001
18. Bonnet F, Cooper ME, Kawachi H, Allen TJ, Boner G, Cao Z: Irbesartan normalises the deficiency in glomerular nephrin expression in a model of diabetes and hypertension. *Diabetologia* 44:874–877, 2001
19. Doublier S, Salvidio G, Lupia E, Ruotsalainen V, Verzola D, Deferrari G, Camussi G: Nephrin expression is reduced in human diabetic nephropathy: evidence for a distinct role for glycated albumin and angiotensin II. *Diabetes* 52:1023–1030, 2003
20. Folkman J: Anti-angiogenesis: new concept for therapy of solid tumors. *Ann Surg* 175:409–416, 1972
21. Folkman J: Angiogenesis in cancer, vascular, rheumatoid and other disease. *Nat Med* 1:27–31, 1995
22. Nyengaard JR, Rasch R: The impact of experimental diabetes mellitus in rats on glomerular capillary number and sizes. *Diabetologia* 36:189–194, 1993
23. Prockop DJ, Kivirikko KI: Collagens: molecular biology, diseases, and potentials for therapy. *Annu Rev Biochem* 64:403–434, 1995
24. Timpl R: Macromolecular organization of basement membranes. *Curr Opin Cell Biol* 8:618–624, 1996
25. Maeshima Y, Colorado PC, Torre A, Holthaus KA, Grunkemeyer JA, Ericksen MB, Hopfer H, Xiao Y, Stillman IE, Kalluri R: Distinct antitumor properties of a type IV collagen domain derived from basement membrane. *J Biol Chem* 275:21340–21348, 2000
26. Maeshima Y, Manfredi M, Reimer C, Holthaus KA, Hopfer H, Chandamuri BR, Kharbanda S, Kalluri R: Identification of the anti-angiogenic site within

vascular basement membrane-derived tumstatin. *J Biol Chem* 276:15240–15248, 2001
27. Maeshima Y, Yerramalla UL, Dhanabal M, Holthaus KA, Barbashov S, Kharbanda S, Reimer C, Manfredi M, Dickerson WM, Kalluri R: Extracellular matrix-derived peptide binds to alpha(v)beta(3) integrin and inhibits angiogenesis. *J Biol Chem* 276:31959–31968, 2001
28. Maeshima Y, Colorado PC, Kalluri R: Two RGD-independent alpha vbeta 3 integrin binding sites on tumstatin regulate distinct anti-tumor properties. *J Biol Chem* 275:23745–23750, 2000
29. Maeshima Y, Sudhakar A, Lively JC, Ueki K, Kharbanda S, Kahn CR, Sonenberg N, Hynes RO, Kalluri R: Tumstatin, an endothelial cell-specific inhibitor of protein synthesis. *Science* 295:140–143, 2002
30. Fossati P, Prencipe L, Berti G: Enzymic creatinine assay: a new colorimetric method based on hydrogen peroxide measurement. *Clin Chem* 29: 1494–1496, 1983
31. Okada S, Shikata K, Matsuda M, Ogawa D, Usui H, Kido Y, Nagase R, Wada J, Shikata Y, Makino H: Intercellular adhesion molecule-1-deficient mice are resistant against renal injury after induction of diabetes. *Diabetes* 52:2586–2593, 2003
32. Weibel ER: Stereological methods. In *Practical Methods for Biological Morphometry*. London, Academic, 1979, p. 51–57
33. Maeshima Y, Kashihara N, Yasuda T, Sugiyama H, Sekikawa T, Okamoto K, Kanao K, Watanabe Y, Kanwar YS, Makino H: Inhibition of mesangial cell proliferation by E2F decoy oligodeoxynucleotide in vitro and in vivo. *J Clin Invest* 101:2589–2597, 1998
34. Sugiyama H, Kashihara N, Makino H, Yamasaki Y, Ota A: Apoptosis in glomerular sclerosis. *Kidney Int* 49:103–111, 1996
35. Kalluri R, Sukhatme VP: Fibrosis and angiogenesis. *Curr Opin Nephrol Hypertens* 9:413–418, 2000
36. Ferrara N: Role of vascular endothelial growth factor in the regulation of angiogenesis. *Kidney Int* 56:794–814, 1999
37. Treins C, Giorgetti-Peraldi S, Murdaca J, Van Obberghen E: Regulation of vascular endothelial growth factor expression by advanced glycation end products. *J Biol Chem* 276:43836–43841, 2001
38. Joussen AM, Poulaki V, Tsujikawa A, Qin W, Qaum T, Xu Q, Moromizato Y, Bursell SE, Wiegand SJ, Rudge J, Ioffe E, Yancopoulos GD, Adamis AP: Suppression of diabetic retinopathy with angiopoietin-1. *Am J Pathol* 160:1683–1693, 2002
39. Sudhakar A, Sugimoto H, Yang C, Lively J, Zeisberg M, Kalluri R: Human tumstatin and human endostatin exhibit distinct antiangiogenic activities mediated by alpha v beta 3 and alpha 5 beta 1 integrins. *Proc Natl Acad Sci U S A* 100:4766–4771, 2003
40. Kalluri R, Shield CF, Todd P, Hudson BG, Neilson EG: Isoform switching of type IV collagen is developmentally arrested in X-linked Alport syndrome leading to increased susceptibility of renal basement membranes to endoproteolysis. *J Clin Invest* 99:2470–2478, 1997
41. Okuda S, Languino LR, Ruoslahti E, Border WA: Elevated expression of transforming growth factor-beta and proteoglycan production in experimental glomerulonephritis: possible role in expansion of the mesangial extracellular matrix. *J Clin Invest* 86:453–462, 1990
42. Senthil D, Choudhury GG, McLaurin C, Kasinath BS: Vascular endothelial growth factor induces protein synthesis in renal epithelial cells: a potential role in diabetic nephropathy. *Kidney Int* 64:468–479, 2003
43. Holzman LB, St John PL, Kovari IA, Verma R, Holthofer H, Abrahamson DR: Nephrin localizes to the slit pore of the glomerular epithelial cell. *Kidney Int* 56:1481–1491, 1999
44. Doublier S, Ruotsalainen V, Salvidio G, Lupia E, Biancone L, Conaldi PG, Reponen P, Tryggvason K, Camussi G: Nephrin redistribution on podocytes is a potential mechanism for proteinuria in patients with primary acquired nephrotic syndrome. *Am J Pathol* 158:1723–1731, 2001
45. Forbes JM, Bonnet F, Russo LM, Burns WC, Cao Z, Candido R, Kawachi H, Allen TJ, Cooper ME, Jerums G, Osicka TM: Modulation of nephrin in the diabetic kidney: association with systemic hypertension and increasing albuminuria. *J Hypertens* 20:985–992, 2002
46. Holthofer H, Ahola H, Solin ML, Wang S, Palmen T, Luimula P, Miettinen A, Kerjaschki D: Nephrin localizes at the podocyte filtration slit area and is characteristically spliced in the human kidney. *Am J Pathol* 155:1681–1687, 1999
47. Eremina V, Sood M, Haigh J, Nagy A, Lajoie G, Ferrara N, Gerber HP, Kikkawa Y, Miner JH, Quaggin SE: Glomerular-specific alterations of VEGF-A expression lead to distinct congenital and acquired renal diseases. *J Clin Invest* 111:707–716, 2003
48. Satchell SC, Harper SJ, Tooke JE, Kerjaschki D, Saleem MA, Mathieson PW: Human podocytes express angiopoietin 1, a potential regulator of glomerular vascular endothelial growth factor. *J Am Soc Nephrol* 13:544–550, 2002